Numerical investigation of the path of a freely vibrating circular cylinder at high reduced frequency value

Dániel Dorogi[1] and László Baranyi[2]
[1,2]Department of Fluid and Heat Engineering, University of Miskolc
[1,2]3515 Miskolc-Egyetemváros, Hungary
[1]aramdd@uni-miskolc.hu, [2]arambl@uni-miskolc.hu

Abstract
Flow around a freely vibrating circular cylinder at high natural frequency is studied numerically. The appearance of a raindrop-shaped cylinder path is found where streamwise oscillation amplitude or time-mean of lift approaches relatively high values. Abrupt jumps are identified in the time-mean of lift when plotted against Reynolds number. Applying developed flows as initial conditions, the range of raindrop-shaped motion increases and jumps in the time-mean of lift disappear.

1. Introduction

Fluid flow around a circular cylinder has been frequently investigated in the past few decades due to its practical importance. When structures such as risers, pipelines and underwater structures are exposed to wind or waves, vortices may shed from the body periodically, causing high amplitude vibrations. An elastically supported cylinder model is commonly used to study free cylinder oscillation. Some investigations deal with one-degree-of-freedom motion (for example Khalak and Williamson, 1999; Willden and Graham, 2006), but more often the cylinder is allowed to move in both streamwise and transverse directions.

Reynolds number $\mathrm{Re}=U_\infty D/\nu$ and reduced velocity $U^*=U_\infty/(f_N D)$ influence the flow significantly, (where U_∞ is the free-stream velocity, ν is the kinematic viscosity of the fluid, D is cylinder diameter and f_N is the natural frequency of the oscillating body). Sing and Mittal (2005) investigated their separate effects at low Reynolds numbers. A two-branch cylinder response (initial and lower branches) was identified, similar to the results obtained by Leontini et al. (2006) for transverse-only motion. In reality, Re and U^* are not independent variables. Assuming that the natural frequency of the body is constant, $\mathrm{Re}=KU^*$ where $K=D^2 f_N/\nu$ is the reduced frequency value. Mittal and Singh (2005) carried out computations for K=3.1875 and found that vortex-induced vibration (VIV) occurs as low as Re≅20, which is a steady-state regime for a stationary cylinder. Prasanth and Mittal (2008) investigated K=16.6 and a significant effect of blockage ratio (the ratio of cylinder diameter and the height of the computational domain) was identified. Kang et al. (2016) reported different cylinder paths such as distorted figure-8, egg-shaped and raindrop-shaped motions.

To the best knowledge of the authors, cylinder response at high natural frequencies and low Reynolds numbers has not been investigated. In this study systematic computations are carried out for the investigation of cylinder paths and aerodynamic force coefficients at the reduced frequency and mass ratio values of (K; m^*)=(40.65; 10). The effect of initial conditions (potential developed flow at different Reynolds numbers) is also analyzed.

2. Governing equations and computational setup

The governing equations for the two-dimensional, incompressible, Newtonian, constant property fluid flow around a freely vibrating circular cylinder are the two components of the Navier-Stokes equations, continuity equation and pressure Poisson equation. Solving for the temporal cylinder displacements, velocity and acceleration components, two structural equations are used (see Khalak and Williamson, 1999).

In order to avoid numerical inaccuracies, the governing equations and the boundary conditions are transformed into the computational domain where the equations are solved using the finite difference method (Baranyi, 2008). The in-house code is thoroughly tested and validated against the available experimental and numerical results for stationary cylinders and forced cylinder motions (see Baranyi, 2008). The results obtained from the free vibration model also show good agreement with the data available in the literature.

In this paper systematic computations are carried out for the investigation of cylinder path and aerodynamic force coefficients at high constant natural frequency corresponding to K≅40.65 (assuming that U^*=4.92, the value used by Singh and Mittal (2005), at Re=200, the reduced frequency value can be obtained as $K=\mathrm{Re}/U^*=200/4.92\cong 40.65$). The mass ratio is fixed at m^*=10

and the structural damping coefficient is set to zero to produce high amplitude vibrations. The effect of initial conditions is also analyzed. Potential and developed flows at different Reynolds numbers are considered as initial conditions.

3. Results and discussion

In Fig. 1a and b root-mean-square (rms) values of streamwise and transverse displacement components (x_{0rms} and y_{0rms}) are shown. Potential flow is set to be the initial condition of the computations. The cylinder response shows two-branch behavior: an initial branch with low cylinder displacements and a lower branch with relatively high oscillation amplitudes. In the Reynolds number range Re≅190–200 x_{0rms} increases suddenly (up to x_{0rms}≅0.022 shown in Fig. 1a), then drops abruptly to lower values. The transverse oscillation amplitude (see Fig. 1b) differs somewhat, since there is only a small jump in the vicinity of Re=200.

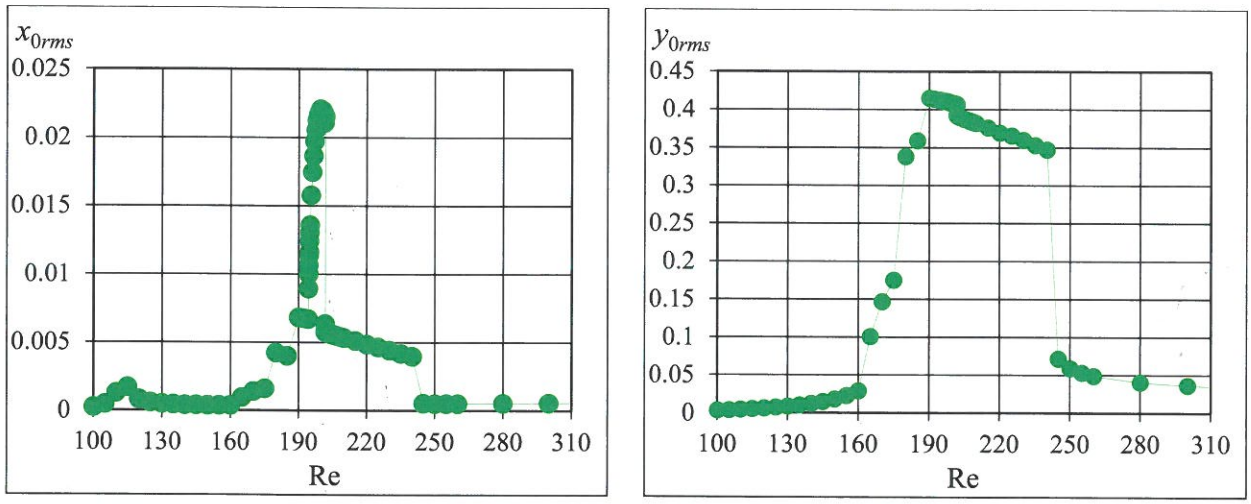

Figure 1: Root-mean-square values of streamwise (a) and transverse (b) cylinder displacements

In the range where x_{0rms} increases significantly, a substantial change in the path of the cylinder is also observed. Using the streamwise to transverse oscillation frequency ratio f_x/f_y shown against Re in Fig. 2b, two different cylinder orbits can be distinguished. At Re<194 and Re>201 the streamwise dimensionless oscillation frequency is double that of the transverse, which leads to a distorted figure-8 motion (see Fig. 2a). In the range of Re=194–201 raindrop-shaped cylinder motion is found, where f_x=f_y (see Fig. 2c). Raindrop-shaped cylinder motion has a significant effect on the lift coefficient. In Fig. 3a the time-mean (TM) of lift C_{Lmean} is plotted against Re. For distorted figure-8 motion its values are approximately zero. As Reynolds number is varied between Re=194 and 201, C_{Lmean} increases. In this range the solution jumps between two so-called state curves that are mirror images of each other. In Fig. 3b lift is shown against drag in the time interval where the flow is periodic. Limit cycles for the pre- and post-jump cases are mirror images of each other.

The vortex structures are also different for distorted figure-8 and raindrop-shaped motions. 2S vortex configuration (two single vortices shed from the body in each motion period) belongs to distorted figure-8 motions (Fig. 4a) while P+S mode (a vortex pair and a single vortex shed) is observed for raindrop-shaped cylinder motions (Fig. 4b).

The question arises how the choice of initial condition influences the cylinder path. For this reason, three different initial conditions are analyzed. One is the potential flow around a circular cylinder, whose results have already been presented in the previous figures. Besides, the developed flows at the Reynolds numbers of Re=192 and 200 and reduced frequency value of K≅40.65 are also set as initial conditions (denoted as Re^1_{init} and Re^2_{init}). Note that at Re=192 distorted figure-8 and at Re=200 raindrop-shaped motions are observed (see in Fig. 2). The results obtained from the computations are shown in Fig. 5. It can be seen that x_{0rms} and C_{Lmean} begin increasing where raindrop-shaped motion occurs and reach higher values in the range of Re=194–207 for Re^1_{init} and Re=194–208 for Re^2_{init} than for figure-8 motion. In addition, these ranges are almost twice as wide for developed flow than the ranges obtained using potential flow as the initial condition. It can also be observed that when using Re^1_{init} and Re^2_{init} the jumps in C_{Lmean} disappear (see in Fig. 5b).

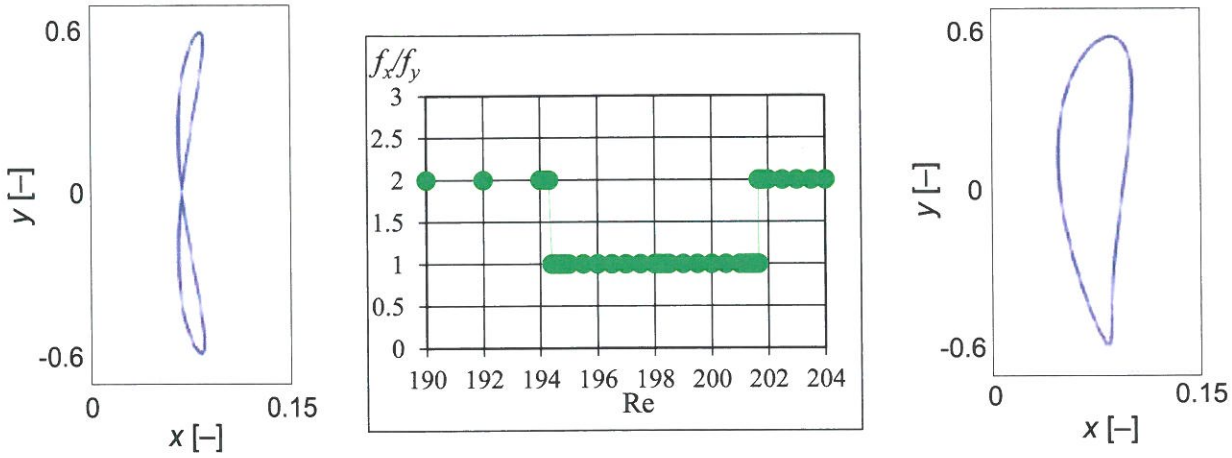

(a) Cylinder path at Re=190 (b) f_x/f_y vs. Re (c) Cylinder path at Re=196

Figure 2: Streamwise to transverse oscillation frequency ratio vs. Re and cylinder paths at two different Reynolds numbers

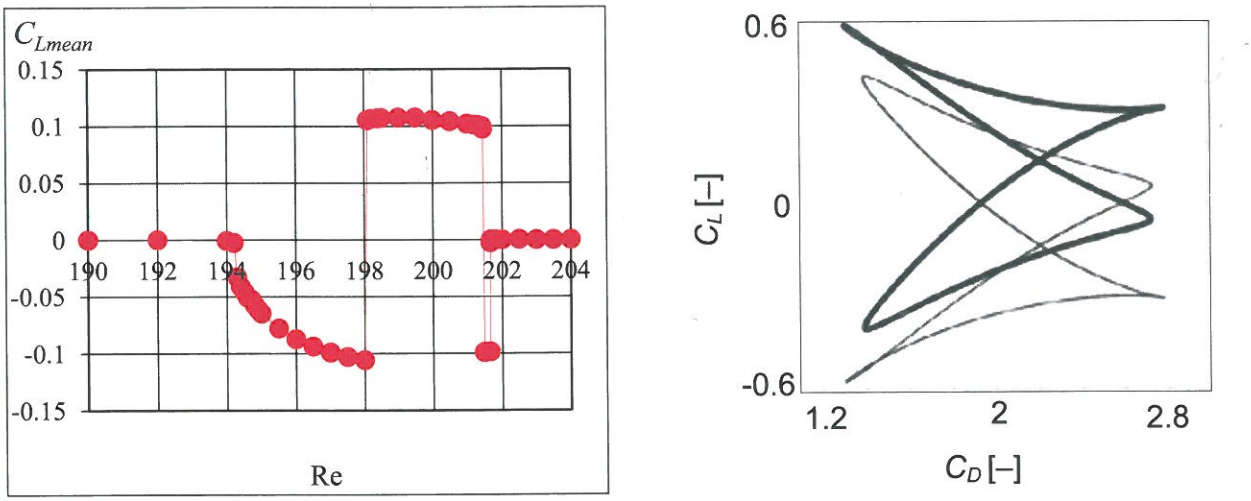

(a) TM of C_L (b) Limit cycles: Re=198 (thin curve); Re=198.1 (thick curve)

Figure 3: Time-mean of lift coefficient vs. Re and (C_D, C_L) limit cycle curves for pre- and post-jump cases

(a) Re=200 (b) Re=204

Figure 4: Vortex structures for distorted figure-8 (a) and raindrop-shaped motions (b)

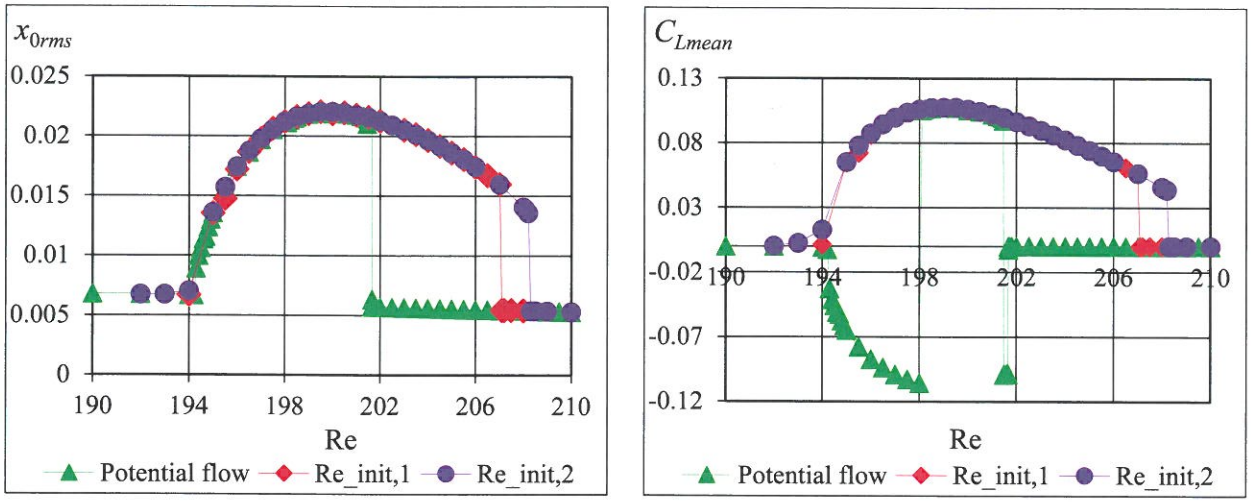

(a) x_{0rms} (b) C_{Lmean}

Figure 5: Rms of streamwise displacement and TM of lift vs. Re for different initial conditions

4. Conclusions

In this study flow around a freely vibrating circular cylinder is investigated numerically for a constant natural frequency corresponding to $K \cong 40.65$. The main findings are:

- the root-mean-square of streamwise displacement (x_{0rms}) and the time mean of lift coefficient (C_{Lmean}) show a gradual increase where figure-8 motion is replaced by raindrop-shaped motion;
- abrupt jumps are found in C_{Lmean} between the two state curves when potential flow around a circular cylinder is set to the initial condition. Using limit cycles it is shown that solutions at the pre- and post-jump cases are mirror images of each other;
- using developed flows at different Reynolds numbers as initial conditions, the raindrop-shaped motion can be maintained in a wider range and the jumps in C_{Lmean} disappear.

Acknowledgement

The research was supported by the EFOP-3.6.1-16-00011 "Younger and Renewing University – Innovative Knowledge City – institutional development of the University of Miskolc aiming at intelligent specialization" project implemented in the framework of the Széchenyi 2020 program. The realization of this project is supported by the European Union, co-financed by the European Social Fund.

References

Baranyi, L., 2008. Numerical simulation of flow around an orbiting cylinder at different ellipticity values. *Journal of Fluids and Structures* **24** (6), 883–906.

Kang, Z., Ni, W., Sun, L., 2016. An experimental investigation of two-degree-of-freedom VIV trajectories of a cylinder at different scales of natural frequency ratios. *Ocean Engineering* **126**, 187–202.

Khalak, A., Williamson, C.H.K., 1999. Motions, forces and mode transitions in vortex-induced vibrations at low mass-damping. *Journal of Fluids and Structures* **13** (7-8), 813–851.

Leontini, J.S., Thompson, M.C., Hourigan, K., 2006. The beginning of branching behavior of vortex-induced vibration during two-dimensional flow. *Journal of Fluids and Structures* **22** (6-7), 857–864.

Mittal, S., Singh, S., 2005. Vortex-induced vibrations at subcritical Re. *Journal of Fluid Mechanics* **534**, 185–194.

Prasanth, T.K., Mittal, S., 2008. Vortex-induced vibrations of a circular cylinder at low Reynolds numbers. *Journal of Fluid Mechanics* **594**, 463–491.

Singh, S.P., Mittal, S., 2005. Vortex-induced oscillations at low Reynolds numbers: hysteresis and vortex-shedding modes. *Journal of Fluids and Structures* **20** (8), 1085–1104.

Willden, R.H.J., Graham, J.M.R., 2006. Three distinct response regimes for transverse vortex-induced vibrations of circular cylinders at low Reynolds numbers. *Journal of Fluids and Structures* **22** (6-7), 885–895.